radiotherapy of human colon carcinoma grafted in nude mice. *Cancer Res* 1995;55: 83–89.
26. Hosono M, Endo K, Hosono MN, et al. Treatment of small-cell lung cancer xenografts with iodine-131-anti-neural cell adhesion molecule monoclonal antibody and evaluation of absorbed dose in tissue. *J Nucl Med* 1994;35:296–300.
27. Wilder RB, McGann JK, Sutherland WR, et al. The hypoxic cytotoxin SR 4233 increases the effectiveness of radioimmunotherapy in mice with human non-Hodgkin's lymphoma xenografts. *Int J Radiat Oncol Biol Phys* 1993;28:119–126.
28. Govindarajulu, Z. *Statistical methods in bioassay.* New York: Karger; 1988:5–6.
29. Dulbecco R, Ginsberg HS. The nature of viruses. In: Davis BD, Dulbecco R, Eisen HN, Ginsberg HS, eds. *Microbiology*, 3rd Ed. Philadelphia: Harper and Row; 1980:883.
30. Berger MJ. Distribution of absorbed dose around point sources of electrons and beta particles in water and other media. *J Nucl Med* 1971;12(suppl 5):5–23.
31. Hui TE, Fisher DR, Kuhn JA, et al. A mouse model for calculating cross-organ beta doses from yttrium-90-labeled immunoconjugates. *Cancer* 1994;73(suppl):951–957.
32. Siegel JA, Wessels BW, Watson EE, et al. Bone marrow dosimetry and toxicity for radioimmunotherapy. *Antibodies Immunoconj Radiopharm* 1990;3:213–233.
33. DeNardo GL, Kukis DL, Shen S, et al. Efficacy and toxicity of ^{67}Cu-2IT-BAT-Lym-1 radioimmunoconjugate in mice implanted with human Burkitt's lymphoma (Raji). *Clin Cancer Res* 1997;3:71–79.
34. Siegel JA, Stabin MG. Absorbed fractions for electrons and beta particles in spheres of various sizes. *J Nucl Med* 1994;35:152–156.
35. Hollander M, Wolfe DA. *Nonparametric statistical methods.* New York: Wiley; 1973:120–123.
36. Agresti A. In: *Categorical data analysis.* New York: Wiley; 1990:283–287.
37. Casarett AP. Acute radiation effects in whole animals. In: Casarett AP, ed. *Radiation biology.* Edgewood Cliffs, NJ: Prentice-Hall; 1968:217–235.
38. Lewis JP, O'Grady LF, Green RA. Clinical and experimental: patterns of exogenous and endogenous hematopoietic repopulation following radiation injury. *J Lab Clin Med* 1977;89:229–239.
39. Thomas GE, Esteban JM, Raubitchek A, Wong JYC. Gamma-interferon administration after ^{90}yttrium radiolabeled antibody therapy: survival and hematopoietic toxicity studies. *Int J Radiat Oncol Biol Phys* 1995;31:529–534.
40. Schmidberger H, Buchsbaum DJ, Blazar BR, Everson P, Vallera DA. Radiotherapy in mice with yttrium-90-labeled anti-Ly1 monoclonal antibody: therapy of the T cell lymphoma EL4. *Cancer Res* 1991;51:1883–1890.
41. Marchese MJ, Zaider M, Hall EJ. Dose-rate effects in normal and malignant cells of human origin. *Br J Radiol* 1987;60:573–576.
42. Juweid M, Neumann R, Paik C, et al. Micropharmacology of monoclonal antibodies in solid tumors: direct experimental evidence for a binding site barrier. *Cancer Res* 1992;52:5144–5153.
43. Boucher Y, Baxter LT, Jain RK. Interstitial pressure gradients in tissue-isolated and subcutaneous tumors: implications for therapy. *Cancer Res* 1990;50:4478–4484.
44. Vaughan ATM, Anderson P, Dykes PW, Chapman CE, Bradwell AR. Limitations to the killing of tumors using radiolabelled antibodies. *Br J Radiol* 1987;60:567–578.
45. Langmuir VK, Fowler JF, Knox SJ, Wessels BW, Sutherland RM, Wong JY. Radiobiology of radiolabeled antibody therapy as applied to tumor dosimetry. *Med Phys* 1993;20(suppl 2):601–610.
46. Kuerbitz SJ, Plunkett BS, Walsh WV, Kastan MB. Wild-type p53 is a cell cycle checkpoint determinant following irradiation. *Proc Natl Acad Sci USA* 1992;89:7491–7495.
47. Lowe SW, Schmitt EM, Smith SW, Osborne BA, Jacks T. p53 is required for radiation-induced apoptosis in mouse thymocytes. *Nature* 1993;362:847–849.
48. Fan S, el-Deiry WS, Bae I, et al. p53 gene mutations are associated with decreased sensitivity of human lymphoma cells to DNA-damaging agents. *Cancer Res* 1994;54: 5824–5830.
49. Harris CC. Structure and function of the p53 tumor suppressor gene: clues for rational cancer therapeutic strategies. *J Natl Cancer Inst* 1996;88:1442–1455.
50. Gu Y, Sarnecki C, Aldape RA, Livingston DJ, Su MSS. Cleavage of poly(ADP-ribose) polymerase by interleukin-1B converting enzyme and its homologs TX and Nedd-2. *J Biol Chem* 1995;270:18715–18718.
51. Lane DP. Cancer. p53, guardian of the genome. *Nature* 1992;358:15–16.
52. Leek RD, Kaklamanis L, Pezzella F, Gatter KC, Harris AL. bcl-2 in normal human breast and carcinoma, association with oestrogen receptor-positive, epidermal growth factor receptor-negative tumours and in situ cancer. *Br J Cancer* 1994;69:135–139.

Technetium-99m-Sestamibi Scintimammography for the Detection of Breast Carcinoma: Comparison Between Planar and SPECT Imaging

Reinhold Tiling, Klaus Tatsch, Harald Sommer, Gabriele Meyer, Martina Pechmann, Katrin Gebauer, Wolfgang Münzing, Rainer Linke, Iraj Khalkhali and Klaus Hahn

Departments of Nuclear Medicine and Gynecology, Klinikum Innenstadt, Ludwig-Maximilians-University, Munich, Germany; and Department of Radiology, Division of Nuclear Medicine, Harbor-University of California, Los Angeles Medical Center, Torrance, California

The purpose of our study was to compare the results of planar and SPECT scintimammography for the detection of breast carcinoma. In addition, our goal was to determine whether SPECT reconstructed with filtered backprojection (FBP) or with iterative algorithms (ISA) can improve the sensitivity and specificity of planar scintimammography (SMM). **Methods:** One hundred thirteen patients with suspicious physical examinations and/or mammography underwent planar lateral and anterior breast imaging as well as SPECT imaging after injection of ^{99m}Tc-sestamibi. We used a blind evaluation, both separately and combined, for planar SMM, ISA-SPECT and FBP-SPECT. Scintigraphic findings were correlated with the final histopathological diagnoses. **Results:** The sensitivity of planar SMM was 80% with a specificity of 83%. All ISA-SPECT studies were of diagnostic quality, while FBP-SPECT was considered nondiagnostic in 14 that were excluded for statistical calculation. Sensitivity of ISA-SPECT and FBP-SPECT were 71% and 69%, respectively. Specificity was 70% for ISA-SPECT and 66% for FBP-SPECT. Combined planar SMM plus ISA-SPECT sensitivity was 85% (81% for planar SMM plus FBP-SPECT) with a specificity of 72%. Three carcinomas indeterminate on planar SMM were correctly identified by combined planar SMM plus ISA-SPECT. ISA-SPECT and FBP-SPECT provided additional information to planar SMM with respect to localization of sestamibi uptake, tumor extent, improved diagnostic certainty and detection of axillary nodes in 40 and 14 patients, respectively. **Conclusion:** ISA reconstruction is the preferable approach to SPECT data. Combined with planar SMM, ISA-SPECT can improve sensitivity. SPECT is useful in cases of indeterminate and positive planar SMM.

Key Words: scintimammography; SPECT; breast imaging; breast carcinoma

J Nucl Med 1998; 39:849–856

Carcinoma of the breast is the most common invasive malignancy in women and the second leading cause of cancer death among women in the U.S. (*1–3*). Since early breast cancer detection reduces mortality and allows breast-conserving surgical therapy, much work has been done to improve early breast cancer detection (*4*). The most succesful screening procedures are breast examinations and mammography, but both have

Received Feb. 1, 1997; revision accepted Aug. 6, 1997.

For correspondence or reprints contact: Reinhold Tiling, MD, Department of Nuclear Medicine, Ludwig-Maximilians-University of Munich, Marchioninistr. 15, 81377 Munich, Germany.

diagnostic limitations. Mammography, while the most effective method with low cost and widespread availability, is less reliable for detecting lesions in dense fibroglandular breasts (*5*). It cannot always accurately differentiate between benign and malignant lesions (*6–8*). To improve sensitivity and specificity of mammography, several different methods such as ultrasonography, digital mammography with computer-aided analysis, MRI and PET of the breast have emerged as useful complementary techniques (*9–12*). In addition, recent articles report promising results for scintigraphy using ^{99m}Tc-sestamibi for the diagnosis of breast carcinoma (*13–20*). Technetium-99m-sestamibi scintimammography (SMM) has been reported to have a high sensitivity (ranging from 79%–96%) as well as a high specificity (ranging from 83%–94%) for the depiction of breast carcinoma in selected populations. These studies have been predominantly performed with high-resolution cameras using the planar imaging technique. There are only a few preliminary observations about the use of SPECT breast imaging (*17,21*). These authors conclude that SPECT imaging is unable to improve diagnostic accuracy of planar SMM for the detection of breast cancer. Although SPECT is reported to assist in the interpretation of difficult planar images and to improve lesion characterization, SPECT is not recommended for routine clinical use (*21*). In the mentioned SPECT studies, filtered backprojection (FBP) was used as a reconstruction technique. Backprojection tends to obscure small lesions with low tracer uptake in the presence of organs with high activity, a situation that is very typical for SPECT SMM. In addition, a single-head detector was used in one of the cited studies (*21*). The technology of imaging systems has been developing rapidly and new multiplicative iterative SPECT reconstruction techniques (MISR) are now available (*22–23*). These techniques were implemented as iterative algorithms (ISA) on Odyssey computer systems (Picker International, Cleveland, OH). ISA is especially useful for the reconstruction of source distributions with very different tracer uptakes.

The goal of our study was to evaluate the role of SPECT performed with a modern dual-head imaging system and to compare SPECT images reconstructed with different algorithms with those of planar imaging.

MATERIALS AND METHODS

Patients

One hundred seventy-four patients (age range 22–81 yr; mean age 51 yr) underwent a physical examination, mammography and ^{99m}Tc-sestamibi SMM between September 1994 and August 1995. One hundred thirteen women in this group with abnormal or indeterminate findings on physical examination and/or mammography had histological confirmation of a lesion. We report our results on this latter group. Physical examination and mammography were performed by an experienced radiologist/gynecologist 2 wk before SMM. Seventy-five patients had indeterminate mammograms and/or clinical examinations, and the remaining 38 patients' findings were suspicious for malignancy (i.e., skin retraction, spiculated mass, clustered linear/branching microcalcifications). Sixty-five patients had palpable and 48 patients had nonpalpable lesions. One hundred twelve patients had histopathologic confirmation by excisional biopsy, lumpectomy or mastectomy within 2 wk of SMM. In only one patient, the fine-needle aspiration cytology result was used as the final diagnosis. Patients with nonpalpable lesions had a prebiopsy localization procedure by using a needle to inject blue dye.

TABLE 1
Interpretation Criteria for Separate Evaluation of Planar SMM and SPECT (ISA/FBP)

Diagnosis	Findings
Normal	Uptake not higher than background
	Diffuse uptake with lower intensity than the upper chest as seen in lateral projection (planar SMM)/sagittal slice orientation (SPECT)
Indeterminate	Diffuse uptake with comparable or higher intensity than the upper chest as seen in lateral projection/sagittal slice orientation
Suspicious	Focal uptake
Nondiagnostic	Image quality does not allow a reliable diagnosis (FBP-SPECT)

SMM = scintimammography; ISA = iterative SPECT algorithm; FBP = filtered backprojection.

Methods

Data Acquisition and Processing

Planar SMM and SPECT were performed prospectively with a dual-head camera system (Prism 2000, Picker International, Cleveland, OH). High-resolution collimators (LEHR) were used. Patients were in the prone position on a foam cushion installed over the image table, which permitted the breast to hang freely. All 115 patients were injected with 20 mCi (740 MBq) ^{99m}Tc-sestamibi into a venous catheter in an antecubital vein in the arm opposite to the breast with the suspected lesion. Five minutes after injection, 10-min planar lateral images of both breasts were acquired simultaneously. This was followed by a 10-min planar anterior image with the patient remaining in the prone position. Planar images were acquired with a matrix size of 256 × 256 pixels. Thirty to 60 min after injection, SPECT was performed. The matrix size of SPECT was 128 × 128 pixels. Data were acquired by a 360° rotation (180 projections, 20 sec/step). SPECT data were reconstructed twice, once using FBP and the second time using ISA with eight iterations. In the FBP, a ramp filter was applied. To remove noise, three-dimensional postfiltering (Butterworth, order 4, cutoff frequency = 0.3 Nyquist) was performed for both techniques. Transverse, sagittal and coronal slices with a slice thickness of one pixel were obtained for both reconstruction techniques.

Image Interpretation

Planar and SPECT images were interpreted by two independent experienced nuclear medicine physicians who were blind to the results of previous diagnostic procedures and to the final histopathologic diagnoses. Sestamibi uptake in planar and SPECT images was visually evaluated separately.

The first-step analysis consisted of a separate evaluation of planar SMM, ISA-SPECT and FBP-SPECT techniques. The criteria for the different scintigraphic diagnoses are outlined in Table 1.

The second-step analysis included interpreting planar images combined with SPECT images. This approach was done twice for ISA-SPECT and separately for FBP-SPECT. The diagnostic criteria for the combined analysis are shown in Table 2. The combination of a suspicious or indeterminate planar SMM with a normal SPECT did not occur. Cases with nondiagnostic SPECT were interpreted according to their planar classification.

The results of both diagnostic approaches, the separate (planar, ISA-SPECT, FBP-SPECT) and the combined reading (planar plus ISA-SPECT, planar plus FBP-SPECT) were compared and correlated with the final histopathologic diagnoses. In addition, the results of the combined approaches were compared with the diagnostic information provided by planar SMM and correlated with histopathologic findings. Scintigraphic classifications of the

TABLE 2
Diagnostic Criteria for Combined Image Reading

Diagnosis		
Negative	Indeterminate	Positive
Normal planar SMM + normal SPECT	Indeterminate planar SMM + indeterminate SPECT	Suspicious planar SMM + suspicious SPECT
Normal planar SMM + indeterminate SPECT	Normal planar SMM + suspicious SPECT	Indeterminate planar SMM + suspicious SPECT
Normal planar SMM + nondiagnostic SPECT	Indeterminate planar SMM + nondiagnostic SPECT	Suspicious planar SMM + nondiagnostic SPECT

SSM = scintimammography; ISA = iterative SPECT algorithm; FBP = filtered backprojection.

two observers were identical except in these cases: (a) planar SMM in one patient; (b) ISA-SPECT in three patients; (c) FBP-SPECT in six patients; (d) planar SMM plus ISA-SPECT in one patient; and (e) planar SMM plus FBP-SPECT in one patient. In these instances, a third nuclear medicine physician acted as a referee and decided the scintigraphic classification.

Statistical Analysis

Sensitivity and specificity of the different approaches were calculated. Statistical evaluation was performed using a chi-square test. A p value < 0.05 was considered statistically significant. An estimation of the sample size and the relative statistical power was performed using nQuery Advisor (Statistical Solutions Ltd., Boston, MA).

RESULTS

There were 59 patients with breast carcinoma in the following pTNM stages: (a) 11 carcinoma in situ; (b) 31 pT1 (3 pT1a, 9 pT1b, 19 pT1c); (c) 13 pT2; (d) 3 pT4; and (e) 1 recurrent carcinoma with a diameter of 1 cm. The mean diameter of infiltrative carcinomas was 18 mm. The smallest tumor was a microscopic focus (diameter 1 mm) of a ductal carcinoma in situ. The remaining 54 patients had these benign lesions: (a) 11 fibroadenomas; (b) 33 fibrocystic diseases; (c) 3 papillomatoses; (d) 1 acute mastitis; (e) 2 chronic mastitis; (f) 3 scars; and (g) 1 intramammary lymph node. Table 3 summarizes the results of all the imaging techniques with respect to their pathologic findings.

In the group with breast carcinoma, planar SMM was suspicious in 47 patients and normal in 7. In 5 patients with carcinoma, planar SMM was indeterminate. Findings of ISA-SPECT and FBP-SPECT were classified as suspicious in 42 and 34 patients, respectively. Three patients with breast carcinoma had normal findings using ISA-SPECT. No patient with carcinoma had normal findings by FBP-SPECT. ISA-SPECT and FBP-SPECT were classified as indeterminate in 14 and 15 patients with carcinoma, respectively.

In the group with benign lesions, planar SMM revealed normal findings in 34 patients. In 9 patients with benign lesions, planar SMM was suspicious. ISA-SPECT and FBP-SPECT showed normal findings in 25 and 15 patients, respectively. SPECT showed suspicious findings in 16 patients using ISA and in 17 patients using FBP. In a total of 14 patients (10 carcinomas, 4 benign lesions), FBP-SPECT was considered nondiagnostic due to the presence of significant artifacts.

The sensitivity and specificity of planar SMM and SPECT are shown in Table 4. When we considered indeterminate findings as negative, ISA-SPECT and FBP-SPECT revealed a sensitivity of 71% and 69%, respectively. These values were

TABLE 3
Results of Planar SMM, ISA-SPECT, FBP-SPECT and Combined Evaluation Correlated with Histopathologic Diagnoses (n = 113)

	Scintimammography (normal/indeterminate/suspicious)				
Histopathology	Planar SMM	ISA-SPECT	FBP-SPECT	Planar plus ISA-SPECT	Planar plus FBP-SPECT
Carcinoma	7/5/47	3/14/42	0/15/34 *10	6/3/50	7/4/48†
Benign diseases	34/11/9	25/13/16	15/18/17 *4	31/8/15	31/7/16†

*Nondiagnostic.
†Cases with nondiagnostic SPECT were read according to planar SMM.
ISA = iterative SPECT algorithm; FBP = filtered backprojection.

TABLE 4
Sensitivity and Specificity of Planar SMM, ISA-SPECT, FBP-SPECT and Combined Evaluation

	Scintimammography				
	Planar	ISA-SPECT	FBP-SPECT	Planar plus ISA-SPECT	Planar plus FBP-SPECT
Sensitivity (%)	80	71†	69*†	85†	81†‡
Specificity (%)	83	70†	66*§	72†	70†‡

*Nondiagnostic cases excluded.
†Cases with nondiagnostic SPECT were read according to planar SMM.
‡p = not significant compared with planar SMM.
§$p < 0.05$ compared with planar SMM.
ISA = iterative SPECT algorithm; FBP = filtered backprojection.

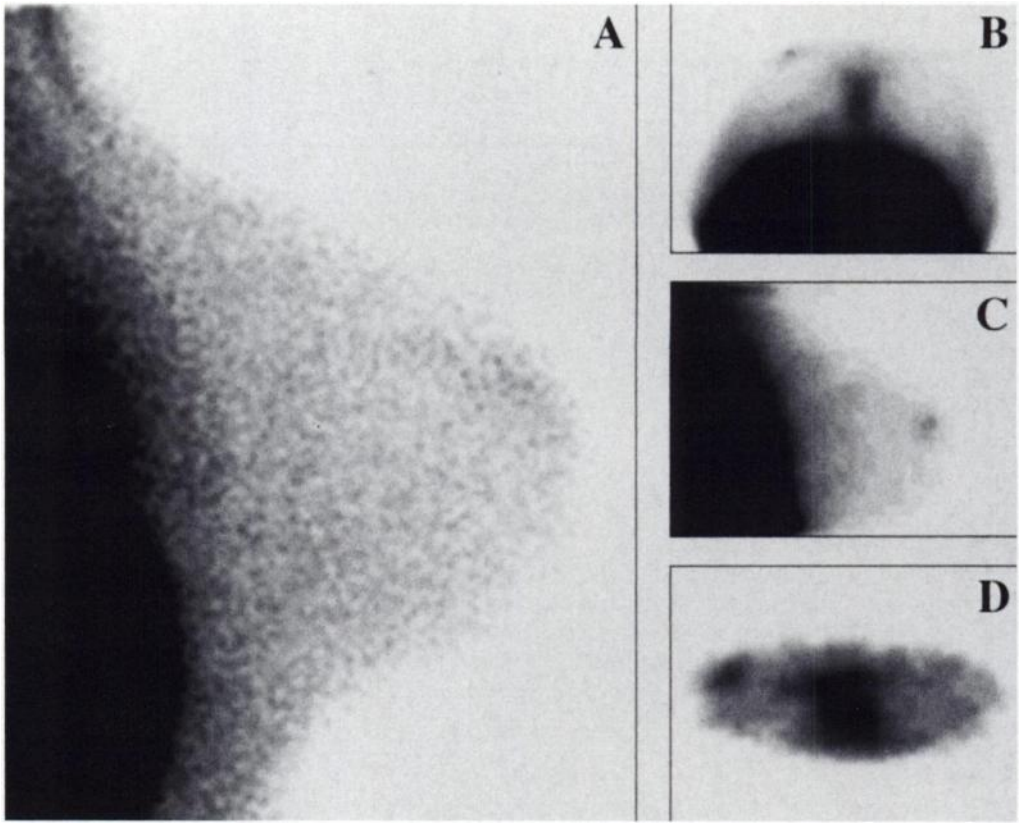

FIGURE 1. Recurrent breast carcinoma with a diameter of 1 cm. (A) Planar lateral SMM was indeterminate, demonstrating area of diffuse uptake in upper breast next to nipple. ISA-SPECT correctly identified carcinoma by focal sestamibi uptake, which was clearly shown in transverse (B), sagittal (C) and coronal (D) slice orientations.

low compared to planar SMM, which had a sensitivity of 80%. The difference, however, was not statistically significant (ISA-SPECT: $p = 0.28$, FBP-SPECT: $p = 0.22$). Specificity was 70% for ISA-SPECT and 66% for FBP-SPECT, respectively. Planar SMM exhibited a specificity of 83%, which was high compared to both SPECT evaluations. The difference was statistically significant compared to FBP-SPECT ($p = 0.04$) but not compared to ISA-SPECT ($p = 0.11$). The results of FBP-SPECT may be biased since all findings classified as nondiagnostic were excluded.

Sensitivity of ISA-SPECT and FBP-SPECT increased significantly ($p < 0.01$) to 95% and 100%, respectively, if indeterminate findings were considered positive. Specificity, however, dropped significantly ($p < 0.01$) to 46% and 37%, respectively. Sensitivity and specificity of planar SMM using this approach were 88% and 63%, respectively. The increase in sensitivity was not significant compared to the approach that considered indeterminate findings as negative ($p = 0.21$). However, the loss in specificity was statistically significant ($p < 0.05$).

Tables 3 and 4 summarize the results of the planar SMM interpretation combined with ISA-SPECT and FBP-SPECT. There were three more carcinomas correctly identified using planar SMM and ISA-SPECT together. These three carcinomas with suspicious findings from ISA-SPECT had indeterminate planar SMM. One of these cases is shown in Figure 1. The combination of planar SMM and FBP-SPECT identified only one of those three carcinomas. On the other hand, 6 of 11 patients with benign disorders who were classified as indeterminate with planar SMM were considered suspicious with the combination planar SMM plus ISA-SPECT. The combination of planar SMM plus FBP-SPECT misinterpreted seven benign diseases as suspicious, and these were classified as indeterminate by planar SMM alone. One patient with breast carcinoma and three patients with benign diseases were classified as normal with planar SMM, but they were classified ultimately as indeterminate using planar SMM plus ISA-SPECT. For planar SMM plus FBP-SPECT, three patients with benign disorders classified as negative by planar SMM were classified as indeterminate using the combined approach.

Considering indeterminate findings as negative, the combination of planar SMM with ISA-SPECT and FBP-SPECT revealed a sensitivity of 85% and 81%, respectively, which was slightly higher than the 80% sensitivity achieved by planar SMM alone. These differences, however, were statistically not significant (planar SMM plus ISA-SPECT: $p = 0.47$, planar SMM plus FBP-SPECT: $p = 0.82$) compared to planar SMM. Specificity of planar SMM plus ISA-SPECT and planar SMM plus FBP-SPECT was 72% and 70%, respectively, which was lower than the specificity of planar SMM alone (83%). Again, differences were statistically not significant (planar SMM plus ISA-SPECT: $p = 0.16$, planar SMM plus FBP-SPECT: $p = 0.11$) compared to planar SMM. The results of planar SMM plus FBP-SPECT may be biased since interpretation of cases with nondiagnostic FBP-SPECT were determined by planar SMM only.

Rating indeterminate findings as positive increased sensitivity of planar SMM plus ISA-SPECT from 85% to 90% (from 81% to 88% for planar SMM plus FBP-SPECT). The increase of sensitivity was not statistically significant (planar SMM plus ISA-SPECT: $p = 0.41$, planar SMM plus FBP-SPECT: $p = 0.31$). Specificity decreased from 72% (ISA) and 70% (FBP) to 57%. The difference was not statistically significant ($p = 0.11$ and $p = 0.16$, respectively).

Beyond the final scintigraphic interpretation concerning the primary tumor, ISA-SPECT and FBP-SPECT provided important additional information in 40 and 14 patients, respectively. Localization of pathologic sestamibi uptake was provided in 28 patients with ISA-SPECT and in 9 patients with FBP-SPECT. In all of these patients, the localization (medial/lateral) of the tumor in planar SMM was impossible due to superimposition of heart or background activity in the planar anterior image (Fig. 2). In 4 patients, either ISA-SPECT or FBP-SPECT enabled

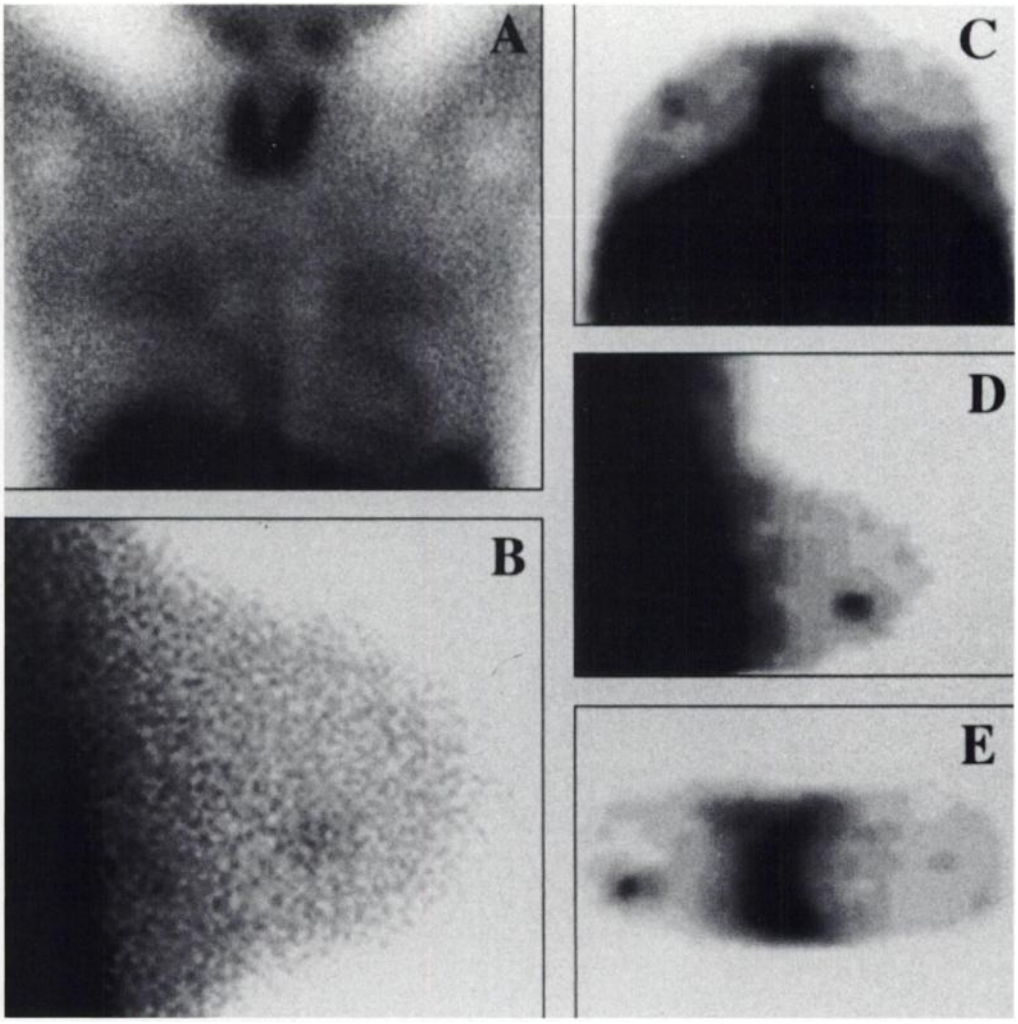

FIGURE 2. Ductal infiltrative carcinoma (pT1c). (A) Planar anterior SMM could not localize faint focal sestamibi accumulation seen on planar lateral image (B) due to superimposition of heart and background activity. ISA-SPECT demonstrated lesion more clearly as shown in transverse (C), sagittal (D) and coronal (E) slice orientations. Exact localization of tumor was possible only by SPECT.

improved assessment of the extent of the tumor compared to planar images (Fig. 3). In the case of faint focal uptake in planar SMM, ISA-SPECT and FBP-SPECT demonstrated the lesion more clearly in 4 patients and 1 patient, respectively. Axillary lymph node metastases were present in 17 patients with breast carcinoma. Focal axillary uptake was noted in 7 of these patients with planar SMM, in 11 with ISA-SPECT and in 6 with FBP-SPECT (Fig. 4). False-positive axillary uptake was seen in 2 patients with planar SMM, in 4 patients with ISA-SPECT and in 7 patients with FBP-SPECT.

DISCUSSION

The positive predictive value of mammography for the detection of breast carcinoma is only 15%–30% for nonpalpable malignancy and 22% for palpable carcinoma (*24–25*). Because of the high number of benign lesions from biopsies resulting from mammographic findings, the use of other complementary techniques may provide additional information on which to base the therapeutic decision. Recent studies suggest a promising clinical role for ^{99m}Tc-sestamibi SMM to aid in the detection of breast carcinoma (*13–20*). These studies were performed using a planar technique and there are only few preliminary reports focusing on the use of SPECT in the detection of breast abnormalities (*17,21*). The authors of these studies conclude that, although some improvement in lesion detection was noticed, tomographic imaging of the breast did not render significant improvement in breast lesion detection. It may be assumed that technical aspects (e.g., imaging device, reconstruction technique) account for the unfavorable results. In contrast with other studies using either a single-head camera system (*21*) or filtered backprojection as the reconstruction technique (*17*), we opted to use a dual-headed camera and to perform different reconstruction methods. We compared planar SMM with the results of the more commonly used method of SPECT reconstruction, FBP, as well with iterative reconstructed slices.

The data comparing SPECT images obtained by FBP with the corresponding images obtained with iterative reconstruction, revealed that ISA-SPECT is superior to FBP-SPECT with a higher specificity (70% versus 66%) without compromising the sensitivity (71% versus 69%). The results of FBP-SPECT compared to ISA-SPECT are less impressive. For example, in 14 patients we observed significant reconstruction artifacts using FBP-SPECT. This group was considered nondiagnostic and was excluded from our study. The calculated results might even be overestimated for FBP-SPECT. In contrast, ISA-SPECT images were diagnostic in all patients. Low count statistics within the breasts and very high activity in organs, such as the heart and liver, included in the reconstruction volume caused artifacts using the FBP technique. These artifacts that are typical and inherent to FBP manifested in scattered stripes overlying the breast. By iterative methods, no such systematic image artifacts are produced. In addition, FBP-SPECT generally resulted in marked inhomogenities of the uptake within the breast. Postfiltering of iterative reconstructed slices is not necessary. However, to minimize the influence of filtering, the same Butterworth filter was applied for both SPECT approaches. Another technical consideration is,

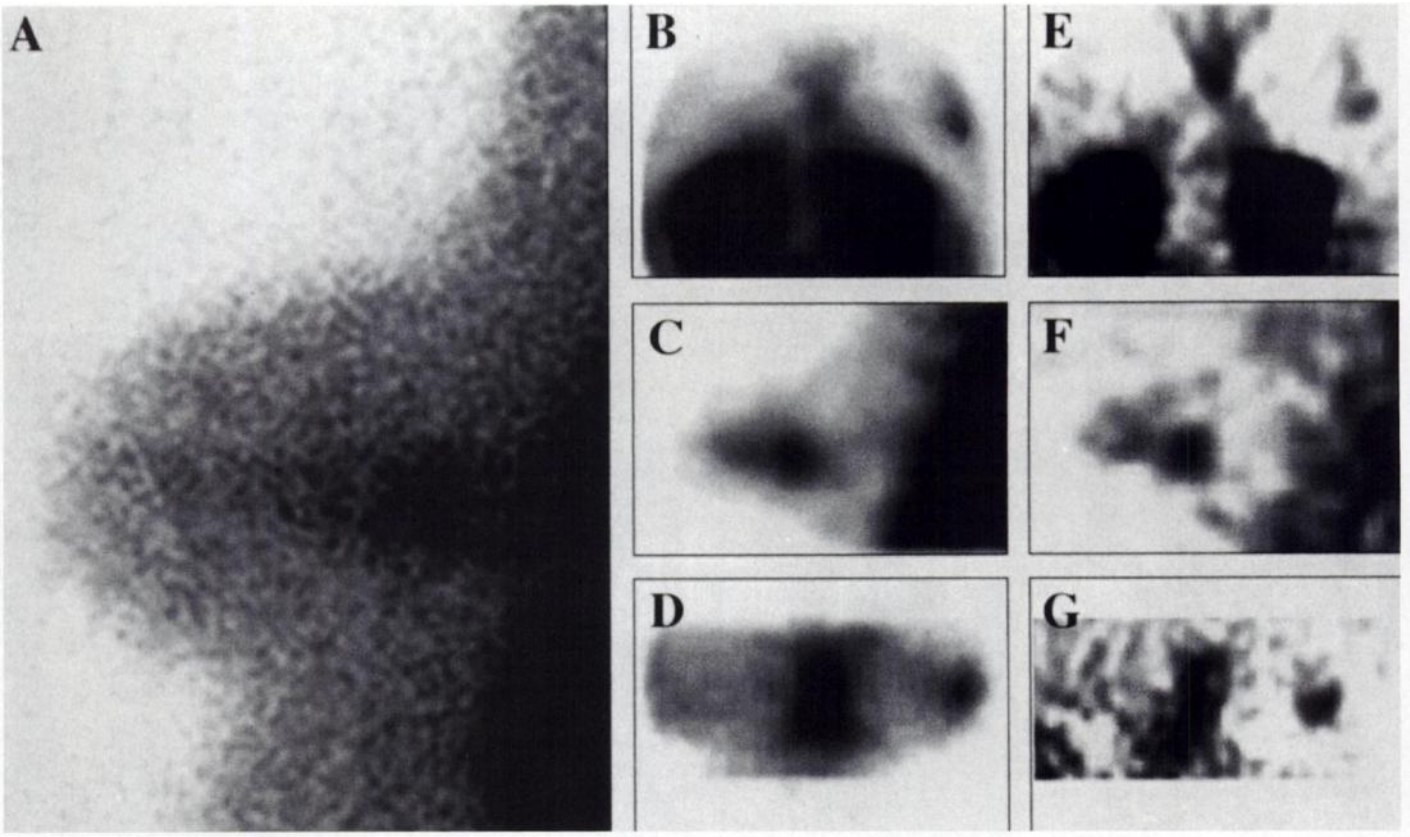

FIGURE 3. Ductal infiltrative carcinoma (pT1b) on basis of extended (3-cm) carcinoma in situ. (A) Planar lateral SMM demonstrated focal sestamibi uptake that could not be delineated from chest wall. Additional transverse (B, E), sagittal (C, F) and coronal (D, G) SPECT slices enabled improved assessment of tumor extent and localization. Diagnostic quality of ISA-SPECT (B–D) was superior due to significant reconstruction artifacts of FBP-SPECT (E–G).

that for SPECT rotation, the detectors are relatively distant from the breasts, which may explain why both SPECT approaches could not reach the diagnostic accuracy of planar SMM (sensitivity = 80%, specificity = 83%).

In evaluating planar SMM combined with SPECT, we found a sensitivity of 85% for planar SMM plus ISA-SPECT and of 81% for planar SMM plus FBP-SPECT. Although the combination of planar SMM and SPECT slightly improved the results of planar imaging alone, the difference based on these results may be not that significant in clinical practice. We note the results of planar SMM plus FBP-SPECT might be overestimated since, in case of nondiagnostic FBP-SPECT, the interpretation of the combined approach was determined by planar SMM only. For the evaluation of planar SMM plus ISA-SPECT, we found that three carcinomas correctly identified by planar SMM plus ISA-SPECT combination had indeterminate planar SMM. One carcinoma was classified as normal in planar SMM and as indeterminate using the planar SMM plus ISA-SPECT combination. This case did not affect the sensitivity since all indeterminate findings were counted as negative. ISA-SPECT, in cases of indeterminate planar SMM, improves the sensitivity. Specificity, however, declines from 83% using planar SMM alone to 72% with planar plus ISA-SPECT and finally to 70% with planar SMM plus FBP-SPECT. In the group of indeterminate planar SMM, the additional interpretation of planar SMM plus ISA-SPECT yielded six more false-positive diagnoses.

Our results were achieved by classifying indeterminate findings of planar SMM and SPECT as negative for carcinoma. The method's sensitivity could be increased significantly (88% for planar SMM, 95% for ISA-SPECT and 90% for the combined evaluation) by considering indeterminate findings as positive. However, this is combined with a decline of specificity to 63% for planar SMM, 46% for ISA-SPECT and 57% for the combined evaluation. This approach is not useful for the clinical routine.

One potential drawback of our study may be the number of cases sampled for statistical analysis. Critical evaluation shows that the relative statistical power of all nonsignificant results we mentioned may be too low (<50%) to rule out the null hypothesis of each comparison (e.g., the null hypothesis that SPECT does not differ in sensitivity or specificity from planar SMM). A sample size of 300-1000 would be required to provide definite proof depending on the calculated p value.

ISA-SPECT compared to FBP-SPECT provided additional diagnostic information concerning the localization and extension of the tumors as well as the presence of axillary lymph node metastases. Concerning the former, planar anterior SMM failed to delineate a focal uptake with low intensity in 28 patients probably a result of superimposition of cardiac or background activity. Thus, we were unable to localize the carcinomas on the anterior view. These patients had clear focal uptake on the SPECT images enabling visualization in different slice orientations. Three-dimensional imaging with SPECT is a promising technique for prebiopsy tumor localization. Such a technique was developed by Mena and Khalkhali et al. (*26–27*). SPECT enabled improved assessment of the tumor extension compared to planar images in four patients. In another four patients, diagnostic certainty was improved with ISA-SPECT. In these cases, only faint focal uptake was noted with planar SMM.

Axillary lymph node metastases were detected in 7 of 17 patients using planar SMM and in 11 of 17 patients with the addition of SPECT using an iterative reconstruction algorithm. However, false-positive interpretations occurred in 2 patients with planar SMM and in 4 patients using ISA-SPECT.

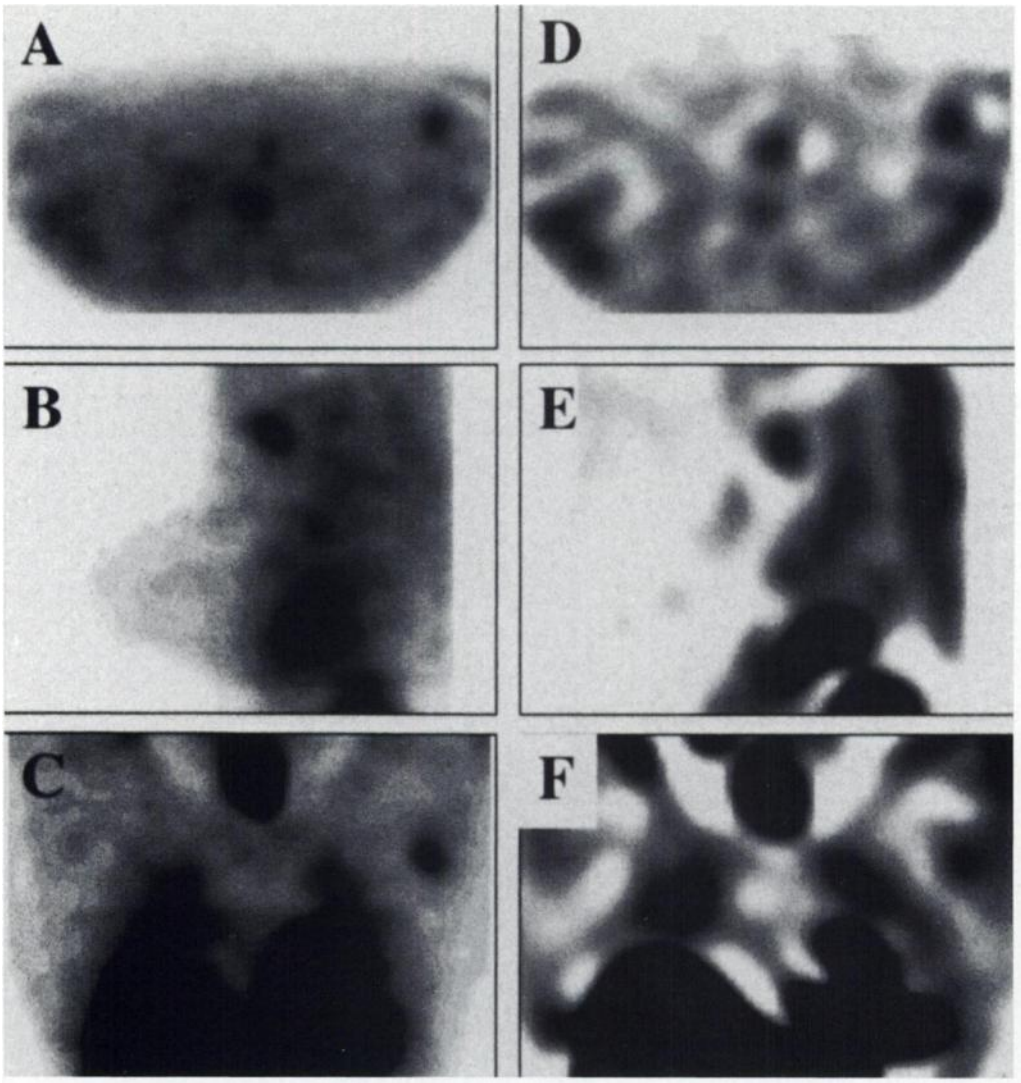

FIGURE 4. Axillary lymph node metastases. ISA-SPECT (A = transverse, B = sagittal, C = coronal slice orientations) clearly demonstrated high intense focal sestamibi accumulation. This finding was also displayed on transverse (D), sagittal (E) and coronal (F) slices of FBP-SPECT. Image quality of FBP-SPECT is inferior compared to ISA-SPECT.

A disadvantage of SPECT versus planar SMM is the additional imaging time required. Older patients and women with conditions that impair their ability to lie quietly are more difficult to image. In addition, performance of ISA requires more sophisticated computers and software that may not be available. Reconstruction time for ISA (depending on hardware, software and imaging parameters) is longer when compared to FBP.

CONCLUSION

ISA-SPECT is the preferable approach to reconstruct SPECT breast imaging data. This method, however, does not improve diagnostic accuracy of planar scintimammography for the detection of breast carcinoma if the SPECT images are evaluated without planar images. The combination of planar SMM plus ISA-SPECT has the potential to improve the sensitivity of planar scintimammography. If planar SMM is negative, the routine use of SPECT is questionable. SPECT imaging contributes unique information for localizing and determining the extent of tumors when there are positive planar scintimammographic findings.

ACKNOWLEDGMENTS

We thank Dr. Fred S. Mishkin, Harbor-UCLA, Los Angeles Medical Center, for advice and assistance in editing the manuscript. We also thank Prof. Dr. Josef Hasford, Institute for Biomathematics, University of Munich, for his help with the statistical analysis.

REFERENCES

1. American Cancer Society. *Cancer facts and figures*. Atlanta, GA: American Cancer Society, 1992.
2. Ries LAG, Hankey BF, Miller BA, Hartman AM, Edwards BK. Cancer statistics review [Abstract]. *J Natl Cancer Inst* 1991;91:2780P.
3. Wingo PA, Tong T, Boldem S. Cancer statistics, 1995. *CA Cancer J Clin* 1995;45: 8–30.
4. Tabar L, Fagerberg CJ, Gad A, et al. Reduction of mortality from breast cancer after mass screening with mammography: randomized trial from the breast cancer screening working group of the Swedish National Board of Health and Welfare. *Lancet* 1985;1:829–832.
5. Jackson VP, Hendrick RE, Kerg SA, et al. Imaging of the radiographically dense breast. *Radiology* 1993;198:297–301.
6. Meyer JE, Sonnenfeld MR, Greenes RA, Stomper PC. Preoperative localization of clinically occult breast lesions: experience at a referral hospital. *Radiology* 1988;169: 627–628.
7. Sickles EA. Mammographic features of 300 consecutive nonpalpable breast cancers. *Am J Roentgenol* 1986;146:661–663.
8. Spivey GH, Perry BW, Clark VA, Coulson AH, Coulson WF. Predicting the risk of cancer at the time of breast biopsy: variation in the benign to malignant ratio. *Am Surg* 1982;48:326–332.
9. Adler DD, Wahl RL. New methods for imaging the breast: techniques, findings, and potential. *Am J Roentgenol* 1995;164:19–30.
10. Avril N, Dose J, Jaenicke F, et al. Metabolic characterization of breast tumors with positron emission tomography using ^{18}F fluordeoxyglucose. *J Clin Oncol* 1996;14: 1848–1857.
11. Harms SE, Flamig DP, Evans WP, Harries SA, Bown S. MR imaging of the breast: current status and future potential. *Am J Roentgenol* 1994;163:1039–1047.
12. Weinreb JC, Newstead G. MR imaging of the breast. *Radiology* 1995;196:593–610.
13. Burak Z, Argon M, Memis A, et al. Evaluation of palpable breast masses with ^{99m}Tc-MIBI: a comparative study with mammography and ultrasonography. *Nucl Med Commun* 1994;15:604–612.
14. Khalkhali I, Mena I, Diggles L. Review of imaging techniques for the diagnosis of breast cancer: a new role of prone scintimammography using technetium-99m sestamibi. *Eur J Nucl Med* 1994;21:357–362.
15. Khalkhali I, Cutrone J, Mena I, et al. Scintimammography: the complementary role of

^{99m}Tc sestamibi prone breast imaging for the diagnosis of breast carcinoma. *Radiology* 1995;196:421–426.
16. Khalkhali I, Cutrone J, Mena I, et al. Technetium-99m-sestamibi scintimammography of breast lesions: clinical and pathological follow-up. *J Nucl Med* 1995;36:1784–1789.
17. Palmedo H, Schomburg A, Grünwald F, Mallmann P, Krebs D, Biersack HJ. Technetium-99m-MIBI scintimammography for suspicious breast lesions. *J Nucl Med* 1996;37:626–630.
18. Taillefer R, Robidoux A, Lambert R, Turpin S, Laperriere J. Technetium-99m-sestamibi prone scintimammography to detect primary breast cancer and axillary lymph node involvement. *J Nucl Med* 1995;36:1758–1765.
19. Tiling R, Sommer H, Pechmann M, et al. Comparison of ^{99m}Tc sestamibi scintimammography with contrast-enhanced MRI for diagnosis of breast lesions. *J Nucl Med* 1997;38:58–62.
20. Waxman A, Nagaraj N, Ashok G, et al. Sensitivity and specificity of ^{99m}Tc methoxy isobutal isonitrile (MIBI) in the evaluation of primary carcinoma of the breast: comparison of palpable and nonpalpable lesions with mammography [Abstract]. *J Nucl Med* 1994;35:22.
21. Diggles L, Khalkhali I. SPECT prone dependent-breast scintimammography [Abstract]. *Eur J Nucl Med* 1994;21:769P.
22. Luig H, Eschner W, Bähre M, Voth E, Nolte G. An iterative strategy for determination of the source distribution in single-photon emission tomography with a rotating gamma camera (SPECT). *Nuklearmedizin* 1988;27:140–146.
23. Luig H, Eschner W, Nolte G, Bähre M, Voth E. In: Schmidt HAE, Csernay L, eds. *Multiplicative iterative SPECT reconstruction (MISR): an approach to exact absorption correction. New trends and possibilities in nuclear medicine.* Stuttgart, New York: Schattauer; 1988:101–104.
24. Kopans DB. The positive predictive value of mammography. *Am J Roentgenol* 1992;158:521–526.
25. Kopans DB. *Breast imaging.* Philadelphia: J.B. Lippincott Co., 1989:320.
26. Mena FJ, Mena I, Diggles LE, Khalkhali I. Design and assessment of a scintigraphy-guided biplane localization technique for breast tumours: a phantom study. *Nucl Med Commun* 1996;17:717–723.
27. Khalkhali I, Mishkin FS, Diggles LE, Klein SR. Radionuclide-guided localization of nonpalpable breast lesions in patients with normal mammograms. *J Nucl Med* 1997;38:1019–1022.

Quantitative Imaging of Iodine-131 Distributions in Brain Tumors with Pinhole SPECT: A Phantom Study

Mark F. Smith, David R. Gilland, R. Edward Coleman and Ronald J. Jaszczak
Departments of Radiology and Biomedical Engineering, Duke University Medical Center, Durham, North Carolina

A method of quantitatively imaging ^{131}I distributions in brain tumors from intratumoral administration of activity was developed and investigated using pinhole SPECT of brain tumor phantoms. **Methods:** Pinhole SPECT sensitivity and resolution were characterized using ^{131}I point-source acquisitions with high-resolution lead (1.4-mm diameter aperture) and tungsten (1.0-mm diameter aperture) pinhole inserts. SPECT scans were obtained from brain tumor phantoms in a water-filled cylinder. The tumor phantoms consisted of spheres filled with an ^{131}I solution to model intratumoral administration of radiolabeled monoclonal antibodies. Two spheres were 20.5 and 97 ml, and two other concentric spheres modeled a tumor with a high-activity shell (71.5 ml) and a low-activity core (21 ml). The collimator focal length was 16 cm and the distance from the pinhole to the center of rotation was 13 cm. The filtered backprojection reconstruction algorithm incorporated scatter and attenuation compensation. SPECT tumor activities and concentrations were estimated using scaling factors from reference point-source scans. **Results:** System sensitivities for point sources at the center of rotation were 28.4 cts/sec^{-1} MBq^{-1} (lead insert) and 13.6 cts/sec^{-1} MBq^{-1} (tungsten insert). SPECT resolutions (FWHM) at the center of rotation were 8.1–11.9 mm (lead) and 6.7–10.3 mm (tungsten). Total tumor activity estimates from SPECT were within 17% of the true activities. SPECT activity concentration estimates in small regions of interest (ROIs) averaged −20% for the 20.5-ml sphere, −11% for the 97-ml sphere, −39% for the shell and +20% for the core of the shell-core phantom. Activity spillover due to limited spatial resolution and the tails of the system response functions biased the estimates. The shell-to-core activity concentration ratio of 4.1 was better estimated with the tungsten insert (2.3) than with the lead insert (1.9) due to better resolution. **Conclusion:** Pinhole SPECT is a promising technique for imaging and quantifying total ^{131}I activity in regions the size of brain tumors. Relative errors were greater for activity concentration estimates in small ROIs than for total activity estimates.

Key Words: pinhole collimator; SPECT; iodine-131 imaging; brain tumor; radioimmunotherapy

J Nucl Med 1998; 39:856–864

The administration of ^{131}I-labeled monoclonal antibodies is a promising strategy for the treatment of malignant tumors (*1,2*). With intratumoral administration of activity, antibody uptake in the tumor is markedly increased relative to intravenous administration (*3,4*). High resolution SPECT imaging will allow the time-dependent three-dimensional accumulation of ^{131}I radiolabeled antibody in the tumors to be followed and will permit better evaluation of tumor dosimetry (*5*). In Phase I studies of ^{131}I radioimmunotherapy at Duke University Medical Center, Durham, NC (*6,7*), 1850–3700 MBq (50–100 mCi) ^{131}I have been administered directly into cystic brain tumors or postoperative resection cavities and intrathecally. We are investigating clinically practical

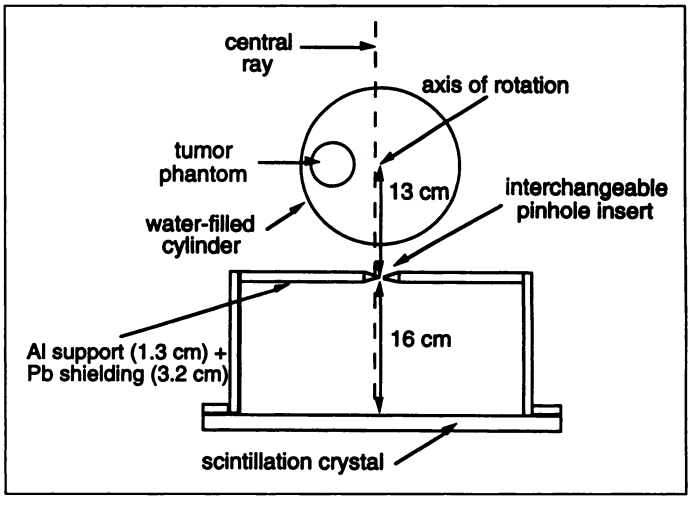

FIGURE 1. Diagram of the pinhole apparatus mounted on one head of a Trionix Triad gamma camera. Also shown is the position of the water-filled cylinder for the SPECT acquisitions and an off-center tumor phantom position.

Received Feb. 1, 1997; revision accepted Jul. 4, 1997.
For correspondence or reprints contact: Mark F. Smith, PhD, National Institutes of Health, Nuclear Medicine Department, Bldg. 10, Rm. 1C401, 10 Center Dr., MSC 1180, Bethesda, MD 20892.